Pergamon

Biochemical Pharmacology, Vol. 49, No. 8, pp. 1099–1110, 1995.

0006-2952/95 $9.50 + 0.00

0006-2952(95)00058-5

CHARACTERIZATION OF THE METABOLIC PATHWAY OF 1,25-DIHYDROXY-16-ENE VITAMIN D_3 IN RAT KIDNEY BY ON-LINE HIGH PERFORMANCE LIQUID CHROMATOGRAPHY–ELECTROSPRAY TANDEM MASS SPECTROMETRY

BERNICE YEUNG,* PAUL VOUROS,*† MEI-LING SIU-CALDERA‡ and G. SATYANARAYANA REDDY‡

*Department of Chemistry and The Barnett Institute, Northeastern University, Boston, MA 02115; and ‡Department of Pediatrics, Women & Infants' Hospital of Rhode Island and Brown University School of Medicine, Providence, RI 02905, U.S.A.

(*Received* 19 *September* 1994; *accepted* 14 *November* 1994)

Abstract—1,25-Dihydroxy-16-ene vitamin D_3 is a synthetic analog of 1,25-dihydroxyvitamin D_3, the most physiologically active metabolite of vitamin D_3. The renal metabolism of 1,25-dihydroxy-16-ene vitamin D_3 had been studied previously using a perfused rat kidney system [Reddy *et al., Bioorg Med Chem Lett* **3**: 1879–1884, 1993], and its C-24 oxidative metabolic pathway had been found to be different from that of 1,25-dihydroxyvitamin D_3 by HPLC. To further delineate the differences between the C-24 oxidative metabolic pathways of 1,25-dihydroxyvitamin D_3 and 1,25-dihydroxy-16-ene vitamin D_3 in this present study we investigated the C-24 oxidation pathway of 1,25-dihydroxy-16-ene vitamin D_3 using a novel detection approach based on on-line capillary liquid chromatography coupled to electrospray tandem mass spectrometry. Two types of tandem mass spectrometric detection were employed to characterize the metabolites in the kidney perfusate: (a) the preliminary screening of metabolites by parent scan, which led to the tentative discovery of the production of 1,23,25-trihydroxy-24-oxo-16-ene vitamin D_3, a new metabolite of 1,25-dihydroxy-16-ene vitamin D_3, and (b) the pharmacokinetic studies of the substrate, 1,25-dihydroxy-16-ene vitamin D_3 and its metabolites by multiple reaction monitoring. In the latter, the mass spectrometric sensitivity for quantification was found to be about 20-fold better than UV detection. The current work concluded that the C-24 oxidative metabolic pathway of 1,25-dihydroxy-16-ene vitamin D_3 closely mimicked that of its natural counterpart. Furthermore, the use of mass spectrometry permitted the clearance rate of the starting substrate to be studied at a more physiological level (ng/mL or submicromolar level), which had not been possible previously by HPLC-UV detection.

Key words: electrospray tandem mass spectrometry; packed capillary liquid chromatography; rat kidney perfusion; pharmacokinetics; chemical derivatization

Vitamin D_3 is a secosteroid synthesized in the skin from 7-dehydrocholesterol upon exposure to sunlight. It is now accepted that vitamin D_3 is hydroxylated in the liver at the C-25 position to form $25(OH)D_3$§, then in the kidney at the C-1 or C-24 positions to form $1,25(OH)_2D_3$ and $24,25(OH)_2D_3$ [1]. Currently, $1,25(OH)_2D_3$ (Scheme 1) is believed to be the most physiologically active form of vitamin D_3 and its role in the maintenance of calcium homeostasis is well established. Research has shown that $1,25(OH)_2D_3$ like other steroid hormones binds to its specific intracellular receptor, which in turn modulates the transcription of various genes [2].

The presence of the $1,25(OH)_2D_3$ receptor has been found in cells that are not involved in calcium metabolism, including the various cancer cell lines, and subsequently it has been discovered that $1,25(OH)_2D_3$ possesses several noncalcemic biological functions [3]. Abe *et al.* [4] for the first time demonstrated the action of $1,25(OH)_2D_3$ on the differentiation of mouse myeloid leukemia cells *in vitro*. Because of this revelation, a great deal of research has been carried out in search of synthetic noncalcemic analogs of $1,25(OH)_2D_3$ that have equal or higher potency in cell differentiation but much

† Corresponding author: Professor Paul Vouros, Department of Chemistry, Northeastern University, 360 Huntington Ave., Boston, MA 02115. Tel. (617) 373-2840; FAX (617) 373-8795

§ Abbreviations: $25(OH)D_3$, 25-hydroxyvitamin D_3; $1,25(OH)_2D_3$, 1α,25-dihydroxyvitamin D_3; $24,25(OH)_2D_3$, 24(*R*),25-dihydroxyvitamin D_3; $\Delta^{16}1,25(OH)_2D_3$, 1α,25-dihydroxy-16-ene vitamin D_3; $\Delta^{16}1,24,25(OH)_3D_3$, 1α,24,25-trihydroxy-16-ene vitamin D_3; $\Delta^{16}1,25(OH)_2$-24-oxo D_3, 1α,25-dihydroxy-24-oxo-16-ene vitamin D_3; $1,25(OH)_2$-24-oxo D_3, 1α,25-dihydroxy-24-oxo-vitamin D_3; $\Delta^{16}1,23,25(OH)_3$-24-oxo D_3, 1α,23,25-trihydroxy-24-oxo-16-ene vitamin D_3; $1,23,25(OH)_3$-24-oxo D_3, 1α,23,25-trihydroxy-24-oxo-vitamin D_3; PTAD, 4-phenyl-1,2,4-triazoline-3,5-dione; μLC, capillary liquid chromatography; TFA, trifluoroacetic acid; ESI, electrospray ionization; MRM, multiple reaction monitoring; and CID, collision-induced dissociation.

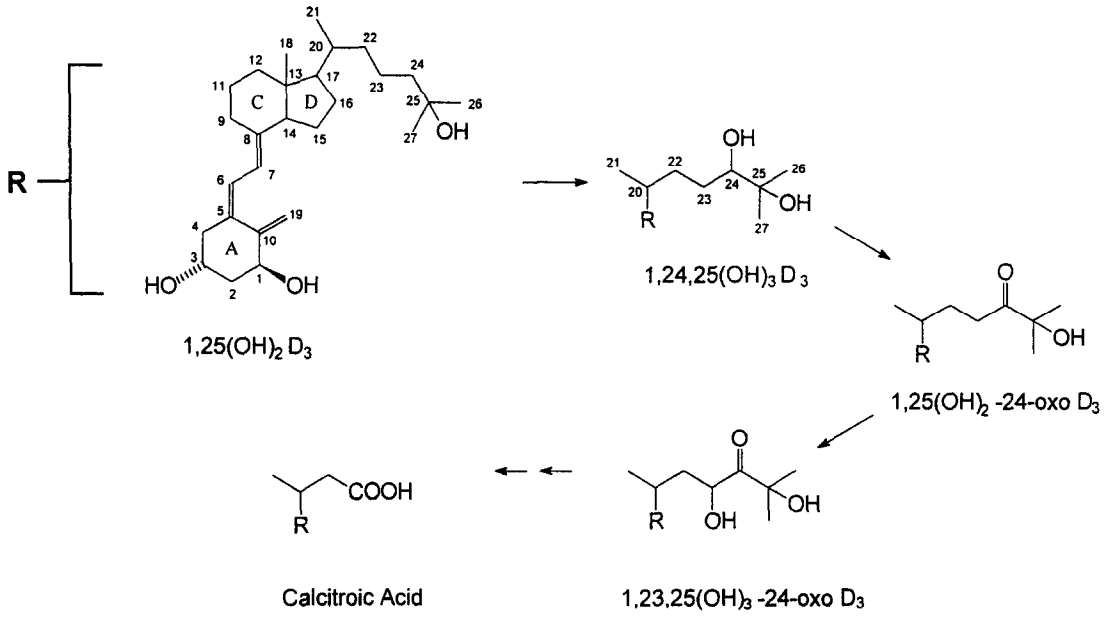

Scheme 1. C-24 oxidative metabolic pathway of $1,25(OH)_2D_3$ in kidney.

lower calcemic effects [5–10]. Several recent studies suggest the possibility of using some of the newly synthesized noncalcemic analogs of $1,25(OH)_2D_3$ as potential drugs in the treatment of psoriasis, cancer, immune disorders and hyperparathyroidism [8, 11–14]. Calcipotriol (MC 903), developed by Leo Pharmaceuticals, has been approved as a drug for the treatment of psoriasis [5, 15–17]. The unique biological activities of the various noncalcemic analogs of $1,25(OH)_2D_3$ may be due to: (a) changes in binding to vitamin D receptor and vitamin D binding protein, and (b) changes in their metabolic pathways and final inactivation in the body. One type of noncalcemic analogs that have received attention includes those that are modified in the D-ring with a 16,17-double bond [7]. In a recent study, $\Delta^{16}1,25(OH)_2D_3$ [Scheme 2, (1)] has been shown as a potent antileukemic agent with low potential to cause hypercalcemia [18]. In an attempt to get a better understanding of the effects of D-ring structural modification on the metabolism of these analogs, Reddy *et al.* [19] studied the metabolic pathway of $\Delta^{16}1,25(OH)_2D_3$ in rat kidney and compared it with that of $1,25(OH)_2D_3$ (Scheme 1). It was concluded that, similar to $1,25(OH)_2D_3$, $\Delta^{16}1,25(OH)_2D_3$ was metabolized into its respective 24-hydroxy and 24-oxo metabolites, but ultimately resisted C-23 hydroxylation. As a result, $\Delta^{16}1,25(OH)_2$-24-oxo-D_3 accumulates as a stable intermediary metabolite when compared with $1,25(OH)_2$-24-oxo-D_3 which is metabolized further into $1,23,25(OH)_3$-24-oxo-D_3. Most recently, it has been demonstrated that $\Delta^{16}1,25(OH)_2$-24-oxo-D_3 is as active as its parent in its immunosuppressive activity, but exhibits less calcemic activity [20]. At present the further metabolic fate of $\Delta^{16}1,25(OH)_2D_3$ is unknown.

In the present work, a novel detection approach

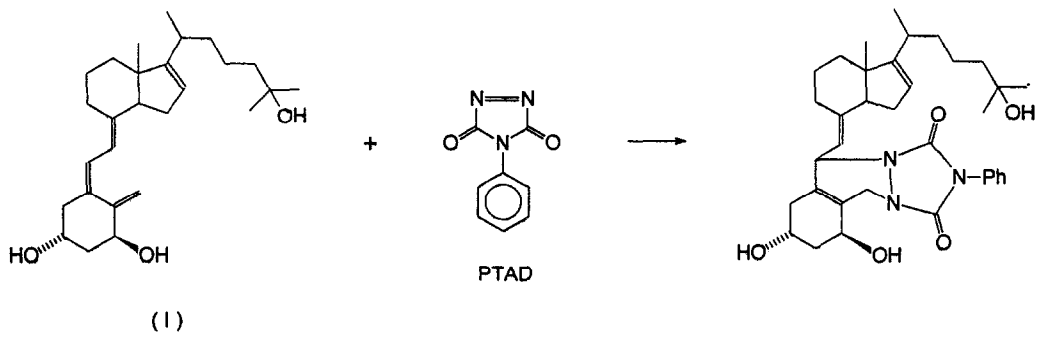

Scheme 2. Derivatization of vitamin D-type compounds by PTAD.

comprised of on-line μLC and tandem mass spectrometry (MS/MS) was utilized for the characterization and detection of the metabolites of $\Delta^{16}1,25(OH)_2D_3$ formed through the C-24 oxidation pathway. Unlike the previous study, rat kidney perfusion experiments of the present study were carried out with lower starting substrate concentrations in order to minimize saturation of the enzymes of the C-24 oxidation pathway. Perfusate samples were first purified by solid phase extraction, and were then subjected to a selective yet simple derivatization reaction with the dienophile PTAD as previously described [21, 22] and illustrated in Scheme 2. The PTAD-derivatized vitamin D compounds were ionized by ESI where their protonated molecular ions (MH^+) underwent facile fragmentation under CID conditions in the mass spectrometer as shown in Scheme 3, resulting in a

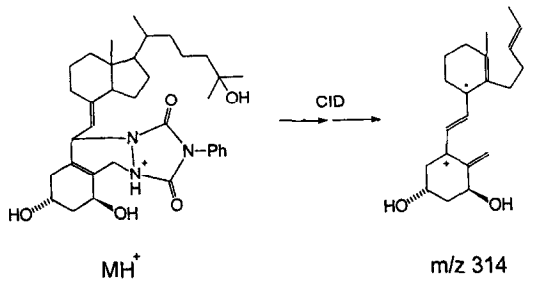

Scheme 3. Fragmentation of MH^+ ion of $1,25(OH)_2D_3$-PTAD to *m/z* 314 under collision-induced dissociation conditions.

characteristic ion transition (MH^+ ---> *m/z* 314) that may be utilized for detection purposes. Based on this unique ion transition, two modes of MS/MS detection were carried out for characterizing the perfusate samples: parent scan, which specifically detected the vitamin D compounds in a mixture and determined their molecular weights, and MRM, which quantified the individual target vitamin D compounds at the trace levels.

MATERIALS AND METHODS

Chemicals

$1,25(OH)_2D_3$ and $\Delta^{16}1,25(OH)_2D_3$ standards were obtained from Dr. M. Uskokovic of Hoffmann-La Roche (Nutley, NJ). The $[^3H]1,25(OH)_2D_3$ tracer (< 1 μCi = < 37 kBq/4 mL) was part of an assay kit obtained from the Nichols Institute (San Juan Capistrano, CA). PTAD was purchased from Aldrich (Milwaukee, WI). Scintilene, Scintiverse II, and HPLC grade acetonitrile and methanol were obtained from Fisher (Pittsburgh, PA). TFA was obtained from Sigma (St. Louis, MO). HPLC grade water was produced in-house by a Milli-Q Plus system (Millipore, Milford, MA).

PTAD-derivatized vitamin D standards

Procedure and reaction conditions were as described before [21, 22].

Rat kidney perfusion

Male Sprague–Dawley rats (375–450 g) (Taconic, Germantown, NY), raised on normal rodent diet sufficient in calcium, phosphorus and vitamin D, were injected with 2 μg of $1,25(OH)_2D_3$ at 20 and 4 hr prior to surgery, in order to achieve maximum renal 24-hydroxylase activity. One kidney was perfused with 100 mL of perfusate containing 8 μg of $\Delta^{16}1,25(OH)_2D_3$, while another kidney was perfused with 100 mL of perfusate containing 80 μg of the substrate, using methodology described previously [23]. Aliquots (5 mL) from each perfusion system were drawn at 10 min, and 1, 2, 3 and 4 hr, after which the perfusion experiments were stopped. The 5-mL aliquots were used to determine the production rates of the metabolites and the clearance rate of the starting substrate by MRM. Twenty-milliliter aliquots were obtained at 4 hr from each perfusion system for the screening of total vitamin D contents by parent scanning.

Solid phase extraction

Two stages of extraction of the perfusate samples using C18 cartridges (500 mg/6 mL; Varian, Sunnyvale, CA) were employed. A vacuum manifold (Alltech, Deerfield, IL) was used for all extraction work. The first stage of the procedure, adapted from a literature method [24], was used for the extraction of analytes from the perfusate. The sample aliquots were collected in borosilicate test tubes and were dried down completely in a Speed-Vac vacuum centrifuge (Savant Instruments, Farmingdale, NY). The dried samples were then reconstituted in 500 μL of acetonitrile, and a solution of PTAD in acetonitrile (20–30 μg/μL) was added dropwise to each tube until the red color persisted. Since the PTAD reagent was added in excess to ensure complete reaction, a second extraction was necessary for its removal so that the chromatography would not be affected. The procedure for this extraction was developed and evaluated using the $[^3H]1,25(OH)_2D_3$ tracer and was as follows: After 30 min of reaction time, each sample aliquot was brought up to 5 mL with H_2O, and the samples were decanted into the reconditioned C18 cartridges. The cartridges were washed with 5 mL of H_2O and 30% acetonitrile under ≈ 0.5 atm (7.4 psi), followed by 4 mL of 100% acetonitrile under ≤ 0.17 atm (2.5 psi), which eluted the PTAD-derivatized analyte. The sample aliquots were collected in 5-mL glass v-vials and were dried to completion in the Speed-Vac. Based on final radioactivity counts of the $[^3H]1,25(OH)_2D_3$ tracer, a 66.1% analyte recovery (relative standard deviation = 2.8%, N = 6) was achieved after all the sample treatment steps as indicated above.

This aforementioned method developed in our laboratory has been used for treating all the perfusate aliquots collected from the rat kidney perfusion experiments. Instead of the tracer, non-radioactive $1,25(OH)_2D_3$ was added as the internal standard and samples were treated in the same fashion. For μLC–

MS/MS analysis, the final dried samples were resuspended in methanol for injection.

μLC conditions

A Carlo Erba Phoenix 20 μLC system (Fisons Instruments, Beverly, MA) was operated in the gradient mode at 5 μL/min as follows: 20% B for 5 min, then up to 100% B in 8 min, held at 100% B for 15 min, where solvent A = H_2O and B = acetonitrile (both with 0.1% TFA). The column was a C18 packed capillary LC column (3 μm, 100 Å particles, 320 μm × 15 cm) (LC Packings, San Francisco, CA). A Rheodyne 7125 injector (Cotati, CA) with a 20-μL PEEK loop was used for all injections, which varied from 1 to 20 μL in volume (in methanol). All separations were carried out at room temperature.

MS conditions

All MS data were obtained on a VG Quattro triple quadrupole mass spectrometer (Fisons Instruments, Beverly, MA) by ESI in the positive ion mode. To maximize intensity of the MH^+ ions of the analytes, the focus lens was set to 10 V and the skimmer lens to 25 V. Source temperature was maintained at 80°, and N_2 was used as both the coaxial gas and the bath gas for desolvation of the droplets. For flow injection work, an Isco μLC-500 pump was used with a carrier solvent of 60% acetonitrile (0.1% TFA) at 5 μL/min. A fused silica capillary (280 μm o.d., 75 μm i.d.) (Polymicro Technologies, Phoenix, AZ) was used for connection between the ESI probe and either solvent pump. For MS/MS, high purity argon was used as the collision gas, and the gas cell pressure was maintained at ≈ 3.8 to 4.3×10^{-3} mbar for MRM and parent scan, and at $\approx 8.0 \times 10^{-4}$ to 1.0×10^{-3} mbar for product ion scan. A collision energy of 20 eV was used for all MS/MS work.

RESULTS

Principles of MS/MS techniques

Before proceeding to the presentation and discussion of results from the rat kidney perfusion experiments, it is appropriate to first define the various MS/MS techniques that were utilized. The three types of MS/MS detection described in this work are product ion scan, parent scan and MRM, all of which are based on the presence of ions (typically including MH^+) in the regular normal scan mass spectrum acquired by ESI. The basic principle behind the MS/MS techniques involves the selection of the appropriate ion (e.g. MH^+), which is admitted into the rf-only mass filter in the second quadrupole of the instrument. Collision of this ion (parent ion) with an inert gas (e.g. argon) then takes place in the collision chamber. Finally, fragment ions resulting from the breakdown of the parent ion are detected in the third quadrupole.

Product ion scan is utilized primarily for structural characterization of an analyte, where the fragment ions formed from the collision of its MH^+ are recorded as a normal scan mass spectrum in the third quadrupole. For a given class of analytes, one or more common fragment ions may be identified from their product ion spectra; such is the case here for the *m/z* 314 ion in the spectra of the derivatized vitamin D compounds. These ions then form the basis of parent scanning, which is used to identify the presence as well as the molecular masses of these analytes. Finally, when the molecular mass of an analyte is known, MRM may be used for more sensitive detection, where the first and the third quadrupoles are set up to transmit only the targeted MH^+ and its selected fragment ion, respectively. In many ways, MRM is analogous to single ion monitoring, which detects only one ion at a specific *m/z*. However, the specificity of MRM is superior since it detects a specific fragmentation involving a pair of ions, rather than only a single ion. MRM data are plotted as a chromatographic peak that represents the abundance of a specific ion transition, which can be used for quantitative purposes. In MRM, multiple ion transitions may be detected and plotted simultaneously, as demonstrated in the following sections. Together these three MS/MS techniques provide a powerful means for the trace level detection and identification of unknown and/or target analytes. For further discussion of these and other MS/MS techniques, readers are referred to Ref. 25.

PTAD-derivatized vitamin D standards

The ESI normal scan mass spectra of $1,25(OH)_2D_3$ and $\Delta^{16}1,25(OH)_2D_3$ standards derivatized by PTAD are shown in Fig. 1. Under conditions that were optimized for MS/MS detection, very little fragmentation was seen for the MH^+ ions in the spectra. Figure 2 shows the product ion spectra of the MH^+ ions of the two PTAD derivatives under CID conditions. In each case, the fragmentation of the MH^+ ions to primarily a single product ion at *m/z* 314 is demonstrated. The ion fragmentation has been described in detail previously [21] and is briefly summarized in Scheme 3. This unique fragmentation pattern, namely MH^+ ---> *m/z* 314, was utilized in all subsequent detections by MS/MS.

Using a μLC on-line with the MS for sample preconcentration, MRM detection of $1,25(OH)_2D_3$-PTAD standard was carried out and is illustrated in Fig. 3. As explained earlier, MRM detects a specific pair of ions in a fragmentation that, in the case of $1,25(OH)_2D_3$-PTAD, was *m/z* 592 (MH^+) ---> *m/z* 314. As shown in Fig. 3, the detection limit for $1,25(OH)_2D_3$ by MRM was *ca.* 50 pg (120 fmol), with a linear response of MRM area counts in the range of 50 pg to 500 ng ($y = 1.2 \cdot 10^3 x + 1.0 \cdot 10^5$, where x = pmol of analyte injected, and y = MRM area counts; N = 2). The error to the estimate was 0.046. The rising baselines seen in parts of Fig. 3 are typical for the trace level detections by MRM, as is the case in the work described in the subsequent sections. It was also observed that peak shapes tended to broaden as the amounts of analytes increased, which was probably caused by: (a) column overloading, and (b) instability of ESI spray when analyte molecules competed for ionization. Nevertheless, the linearities of response as well as the dynamic range of analysis were found to be satisfactory and neither was affected by the peak shapes.

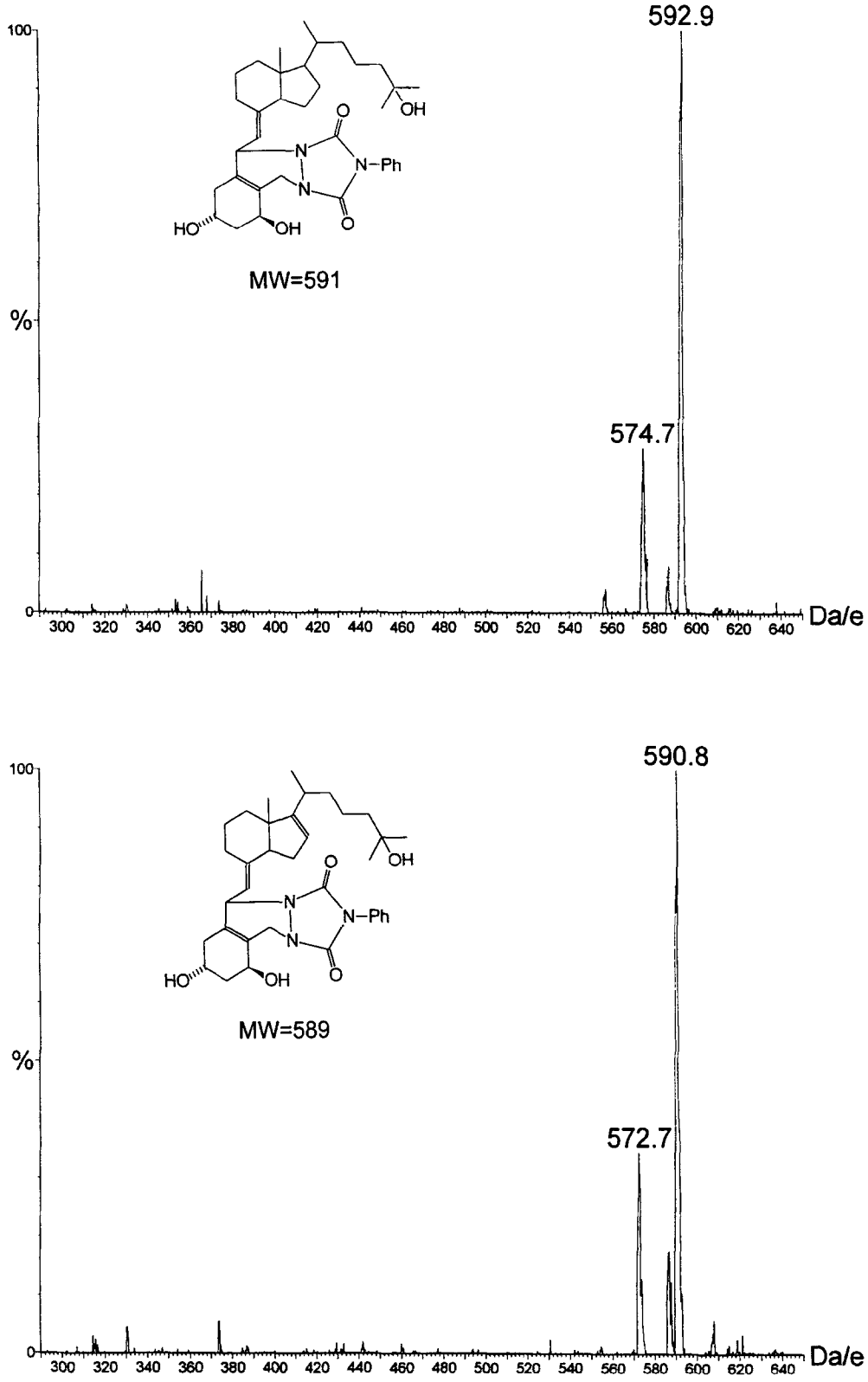

Fig. 1. Electrospray ionization (ESI) normal scan spectra of (top panel) $1,25(OH)_2D_3$-PTAD, 50 ng, with $MH^+ = 592.9$; and (bottom panel) $\Delta^{16}1,25(OH)_2D_3$-PTAD, 50 ng, with $MH^+ = 590.8$. Data were obtained by flow injection analysis.

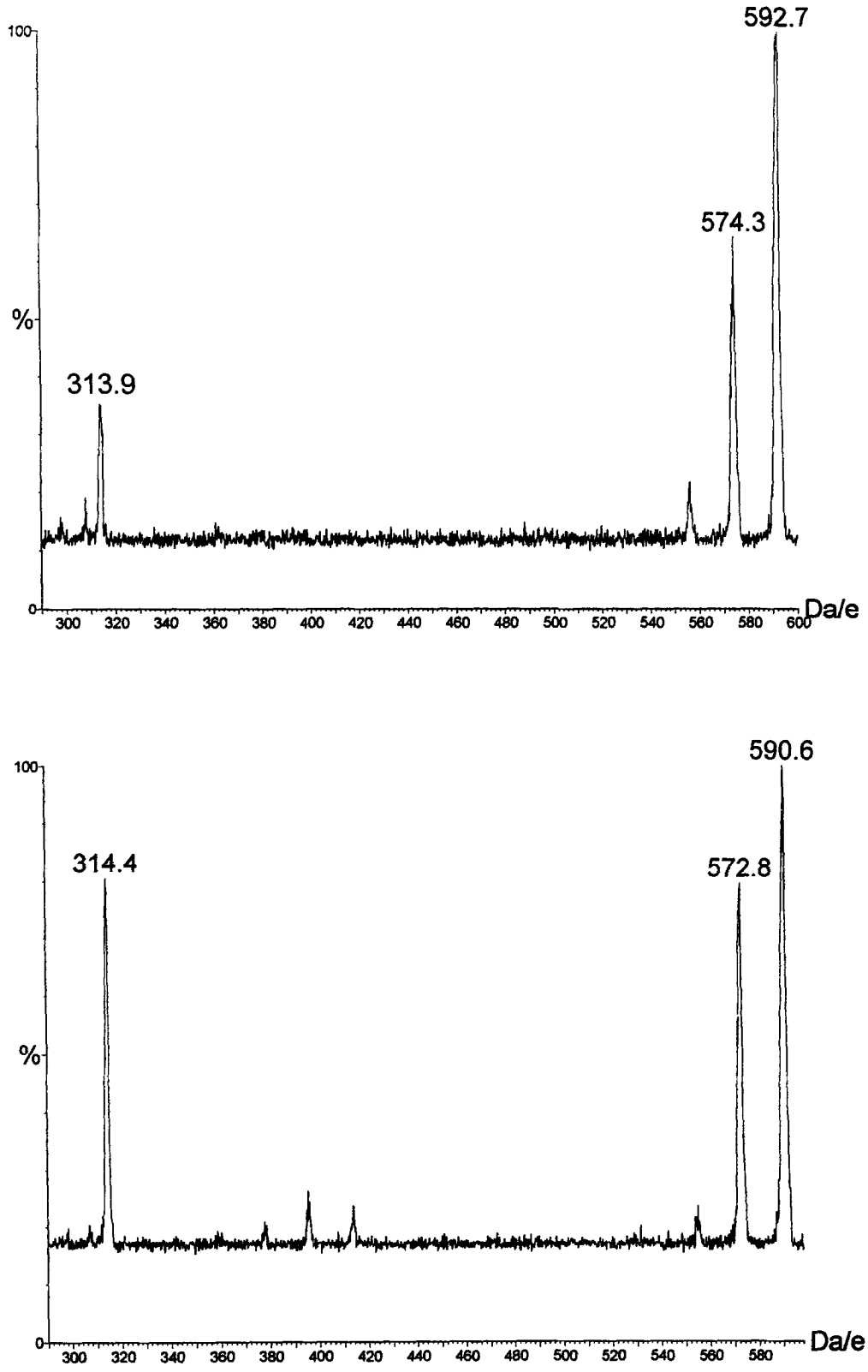

Fig. 2. Product ion spectra of the MH^+ ions of (top panel) $1,25(OH)_2D_3$-PTAD (*m/z* 592.7), 50 ng; and (bottom panel) $\Delta^{16}1,25(OH)_2D_3$-PTAD (*m/z* 590.6), 50 ng. Both were obtained by flow injection analysis.

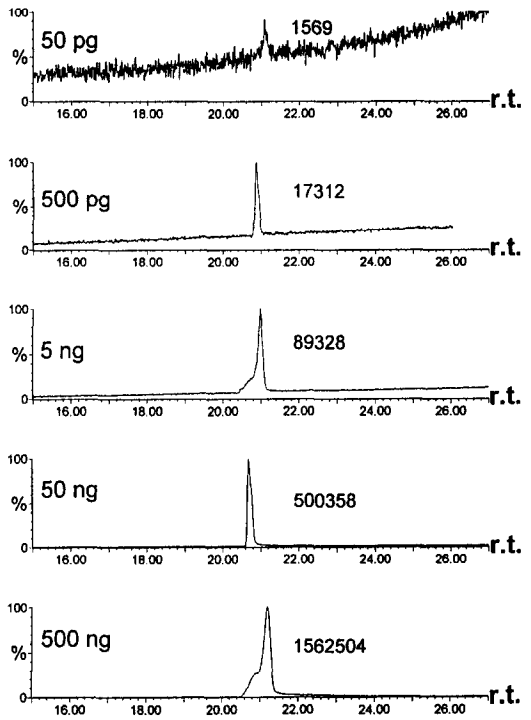

Fig. 3. Multiple reaction monitoring (MRM) analysis of $1,25(OH)_2D_3$-PTAD standard using the ion transition of m/z 592 ---> m/z 314. Data were obtained by μLC-ESI MS/MS and are plotted as a function of retention time (r.t.). Area counts are indicated next to each peak.

Spiked blank perfusate samples

Blank perfusate solutions spiked with various amounts of both $1,25(OH)_2D_3$ and $\Delta^{16}1,25(OH)_2D_3$ standards were prepared and treated as outlined in Materials and Methods. The final dried samples were resuspended in 20 μL of methanol for injections onto the capillary LC column. For MRM detection, two ion transitions were selected for the simultaneous monitoring of both analyses: m/z 592 ---> m/z 314 for $1,25(OH)_2D_3$-PTAD, and m/z 590 ---> m/z 314 for $\Delta^{16}1,25(OH)_2D_3$-PTAD. Figure 4 shows the results of some of these analyses, in the range from 500 pg/mL to 500 ng/mL of each analyte spiked (N = 2). For $1,25(OH)_2D_3$-PTAD, the standard curve was $y = 4.3 \cdot 10^2 x - 6.0 \cdot 10^3$, with an error to the estimate = 0.0025; for $\Delta^{16}1,25(OH)_2D_3$-PTAD, the standard curve was $y = 3.1 \cdot 10^2 x - 5.1 \cdot 10^2$, with an error to the estimate = 0.00015. Similar to the observation with the $1,25(OH)_2D_3$-PTAD standard, the MRM peak shapes obtained with the spiked perfusate also broadened as the amounts of analytes increased.

To evaluate sample recovery during μLC-MS analysis, blank perfusate solutions were purified as described before [24] and then spiked with various amounts of both PTAD-derivatized $1,25(OH)_2D_3$ and $\Delta^{16}1,25(OH)_2D_3$ standards. These samples were examined using the μLC-MS/MS by MRM, and the area counts obtained were compared with those shown in Fig. 4. Comparison of these results (i.e. MRM signals from analyte spiked in sample before

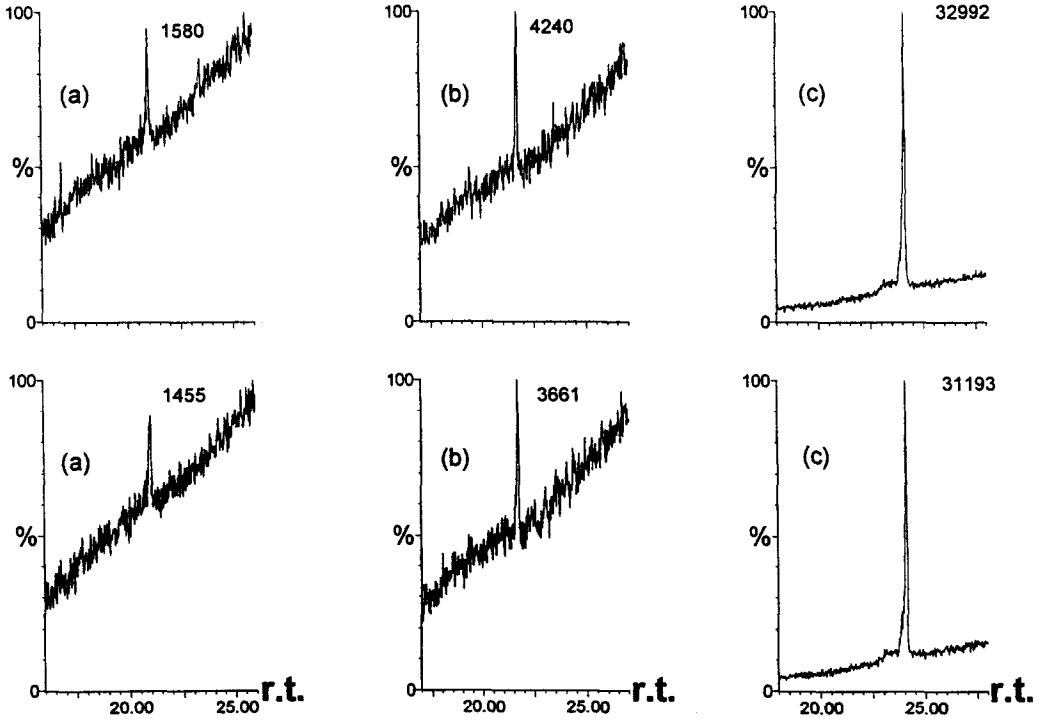

Fig. 4. MRM analysis by μLC-ESI MS/MS of blank perfusate samples spiked with $1,25(OH)_2D_3$ (top traces, m/z 592 ---> m/z 314) and $\Delta^{16}1,25(OH)_2D_3$ (bottom traces, m/z 590 ---> m/z 314). Amounts of both compounds spiked in each mL of perfusate sample: (a) 500 pg; (b) 5 ng; (c) 50 ng. Area counts are indicated.

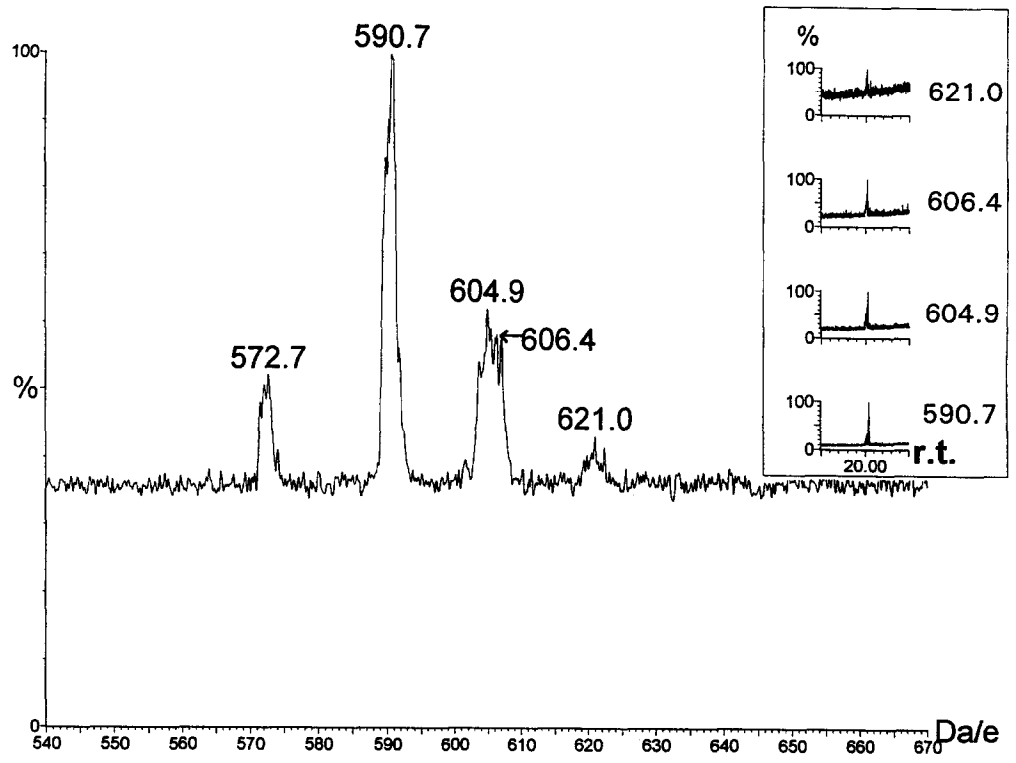

Fig. 5. Identification of metabolites of $\Delta^{16}1,25(OH)_2D_3$ produced in rat kidney by μLC-ESI MS/MS using parent scan on 2 mL of final perfusate. Metabolites were detected as PTAD derivatives and identified as $\Delta^{16}1,25(OH)_2D_3$ (substrate, *m/z* 590.7), $\Delta^{16}1,24,25(OH)_3D_3$ (*m/z* 606.4), $\Delta^{16}1,25(OH)_2$-24-oxo D_3 (*m/z* 604.9) and $\Delta^{16}1,23,25(OH)_3$-24-oxo D_3 (*m/z* 621.0). The reconstructed ion chromatograms of these ions are shown in the inset. *m/z* 572.7 is the loss of H_2O from *m/z* 590.7.

vs after solid phase extraction) revealed average MS signal recoveries of 64% for $1,25(OH)_2D_3$-PTAD and 68% for $\Delta^{16}1,25(OH)_2D_3$-PTAD, which was well in line with the analyte recovery found by radioactivity counting after sample extraction and treatment (see Materials and Methods). These results demonstrated that no significant analyte loss was encountered during the μLC-MS/MS detection. The linearities of detection by MRM of both analytes also established the suitability of $1,25(OH)_2D_3$ as an internal standard for the detection of $\Delta^{16}1,25(OH)_2D_3$ in perfusate. The detection limit by MRM in perfusate was ≈ 500 pg (1.2 pmol) for both analytes.

Perfusate samples from rat kidney perfusion experiment

Parent scan. A 2-ml aliquot from the 80 μg perfusion experiment was prepared as described earlier, and the final sample was injected onto the μLC-MS/MS system and examined by parent scan. As explained earlier, this technique identifies the molecular masses of analytes that fragment to give ions of a specific *m/z*. In this experiment, the third quadrupole of the mass spectrometer was set up to detect only the production of the *m/z* 314 fragment ion after collision, while the first quadrupole was used to scan over a mass range that bracketed the expected MH^+. Based on previous findings [19, 26], a mass range of *m/z* 540 to *m/z* 670 was scanned in the first quadrupole, which would bracket the masses of the MH^+ ions of all possible metabolites produced in the C-24 oxidation pathway (Scheme 1) after derivatization with the PTAD reagent. The parent scan results are shown in Fig. 5, which contains the MH^+ of all C-24 metabolites found previously by Reddy *et al.* [19] ($\Delta^{16}1,24,25(OH)_3D_3$ and $\Delta^{16}1,25(OH)_2$-24-oxo-D_3), as well as an additional C-24 metabolite in minor quantity, corresponding in mass to the PTAD-derivatized $\Delta^{16}1,23,25(OH)_3$-24-oxo-D_3. A 5-mL aliquot from the same sample was examined by conventional HPLC with UV detection, and the chromatogram (Fig. 6) was similar to that obtained in the previous work [19] which, however, had failed to provide evidence for the existence of the third metabolite.

MRM detection. Aliquots (5 mL) from the 80 μg/100 mL perfusion collected at different time points were each spiked with 4 μg of the internal standard $1,25(OH)_2D_3$. After sample clean up and derivatization with PTAD, the final samples were each resuspended in 80 μL of methanol. Four injections were made from each vial of sample onto the μLC-MS/MS system, with each injection containing 1 μg of the internal standard. Rep-

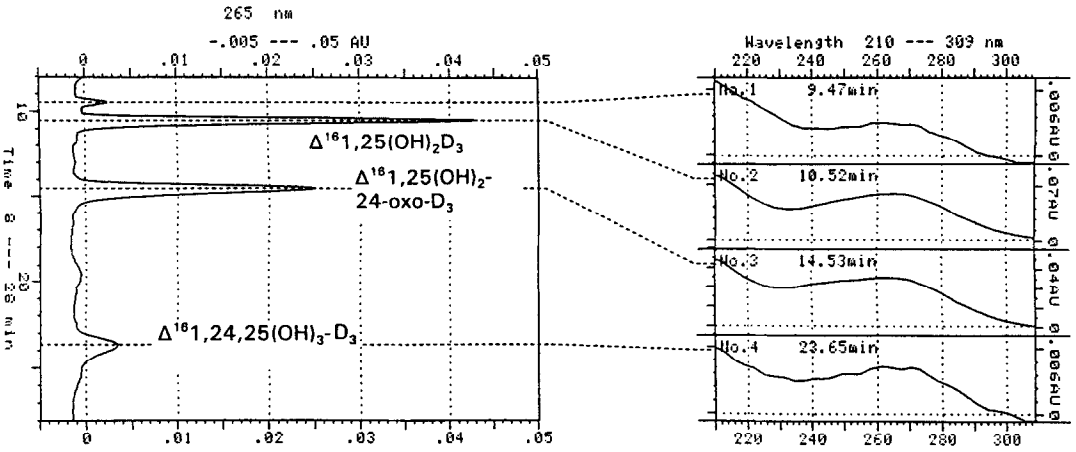

Fig. 6. Identification of metabolites of $\Delta^{16}1,25(OH)_2D_3$ produced in rat kidney by HPLC-UV detection at 265 nm of 5 mL of the final perfusate, identifying the starting substrate, and two C-24 metabolites, $\Delta^{16}1,24,25(OH)_3D_3$ and $\Delta^{16}1,25(OH)_2$-24-oxo D_3. UV spectra of these compounds are also shown. The HPLC system used was a Waters 600 pump with a 900 PDA detector. Isocratic separation was carried out using a Zorbax-SIL column (25 cm × 4.6 cm) with hexane : isopropanol (90 : 10) at 2 mL/min.

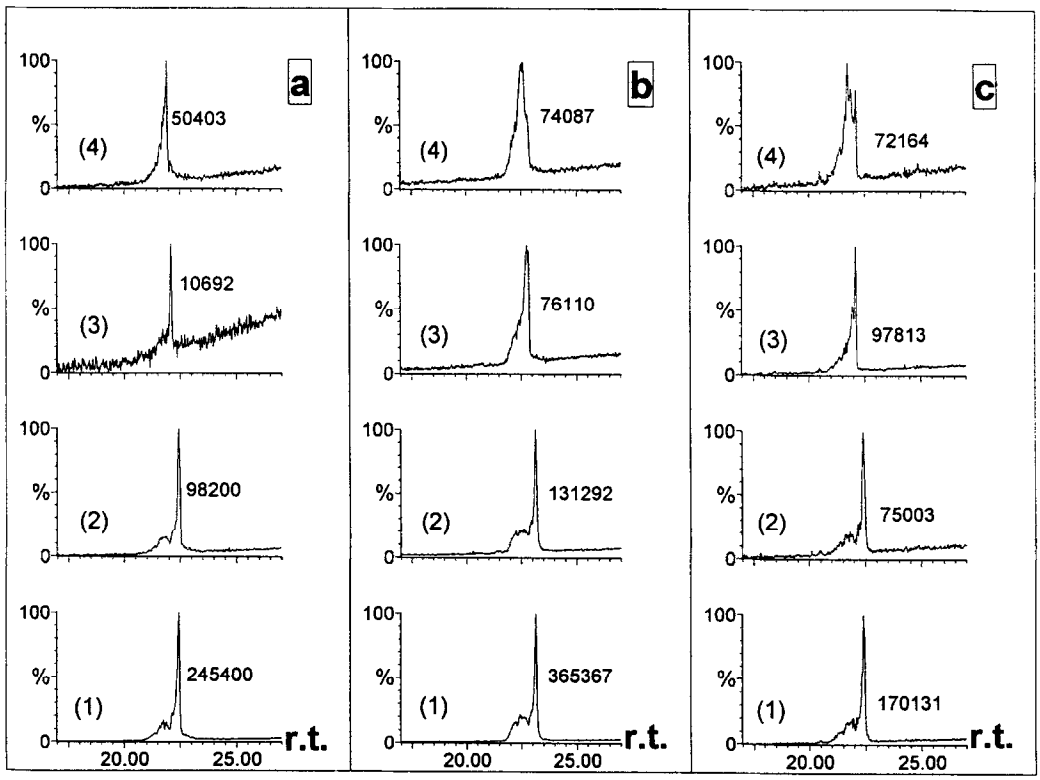

Fig. 7. MRM analysis by μLC-ESI MS/MS of perfusates from the 80 μg/100 mL perfusion experiment, drawn at (a) 10 min; (b) 2 hr; (c) 4 hr. In each figure, trace (1) = $\Delta^{16}1,25(OH)_2D_3$-PTAD (substrate, m/z 590 ---> m/z 314), trace (2) = $1,25(OH)_2D_3$-PTAD (internal standard, m/z 592 ---> 314), trace (3) = $\Delta^{16}1,25(OH)_2$-24-oxo D_3 (m/z 605 ---> m/z 314), and trace (4) = $\Delta^{16}1,24,25(OH)_3D_3$ (m/z 606 ---> m/z 314). All compounds were derivatives of PTAD. Data of perfusates taken at 1 and 3 hr of the perfusion experiment are not shown.

resentative MRM profiles from the μLC-MS/MS analysis at several of the time points are displayed in Fig. 7, which shows the simultaneous detection of the internal standard, the starting substrate and two of the C-24 oxidative metabolites, using ion transitions as indicated in the figure legend. The third C-24 metabolite, discovered by parent scan as described earlier, was not detected by MRM due to its low quantities in these aliquots. Notably, the detection of Δ^{16}1,23,25(OH)$_3$-24-oxo-D$_3$ by parent scan (Fig. 5) was done with the final (4 hr) perfusate when it was present at its highest concentration. The production rates of the two C-24 oxidative metabolites were plotted in Fig. 8.

From the second perfusion experiment using a 8 μg/100 mL starting substrate concentration, 5-mL aliquots collected at each time point were each spiked with 180 ng of 1,25(OH)$_2$D$_3$, and then were extracted and treated with PTAD. Each final sample was reconstituted in 80 μL of methanol, and four injections were made, each containing 45 ng of the internal standard. MRM analyses were carried out simultaneously for the substrate and the internal standard (data not shown), using the appropriate ion transitions as described in the legend of Fig. 7. Based on the area counts observed in the MRM analyses, the half-life ($t_{1/2}$) of Δ^{16}1,25(OH)$_2$D$_3$ was calculated to be 220 min for the 80 μg/100 mL perfusion, and 63 min for the 8 μg/100 mL perfusion. Therefore, the clearance of Δ^{16}1,25(OH)$_2$D$_3$ by the kidney was found to be faster when a lower starting substrate concentration was present.

DISCUSSION

In this study, the utility and feasibility of μLC-ESI MS/MS coupled with a simple chemical derivatization for the analysis of vitamin D metabolites in biological samples were demonstrated. Methods for sample treatment as well as the analytical methodology were developed and applied toward the characterization of the metabolic pathway of Δ^{16}1,25(OH)$_2$D$_3$ in rat kidney. From the parent scan data, it appears that the C-24 oxidation of Δ^{16}1,25(OH)$_2$D$_3$ resembles that of 1,25(OH)$_2$D$_3$, in which the third C-24 oxidative metabolite, Δ^{16}1,23,25(OH)$_3$-24-oxo-D$_3$, is in fact produced in the kidney, albeit in a much smaller quantity. Therefore, contrary to previous results [19], it appears that structural modification in the D-ring of 1,25(OH)$_2$D$_3$ does not alter the sequence of the enzymatic reaction of the C-24 oxidation pathway. It only alters the rate of C-23 hydroxylation of Δ^{16}1,25(OH)$_2$D$_3$. The parent scan results reported here are the first indication of the production of Δ^{16}1,23,25(OH)$_3$-24-oxo-D$_3$ in the kidney. However, further verification of the presence and precise pharmacokinetic measurements of this metabolite are warranted.

Pharmacokinetic studies of the perfusion experiments were also possible using the μLC-MS/MS system. Because of the sensitivity of the technique, small aliquots of perfusate may be drawn at various time points for time–course studies without adversely affecting the overall environment of the kidney perfusion system. The production rates of the C-24 metabolites as well as the $t_{1/2}$ values of the substrate were characterized based on the MRM data obtained. More importantly, the sensitivity of MRM detection allowed the starting substrate concentration to be reduced by ≈ 20-fold over that used previously [19]. The lower concentration (ng/mL or submicromolar) used was significantly closer to physiological conditions, and its $t_{1/2}$ in the kidney, as determined by MRM analysis, was therefore more realistically reflected. As evident from the calculated $t_{1/2}$ values of Δ^{16}1,25(OH)$_2$D$_3$ in the two perfusion experiments, the clearance of the substrate was ≈ 3.5 times faster when a lower starting concentration was present,

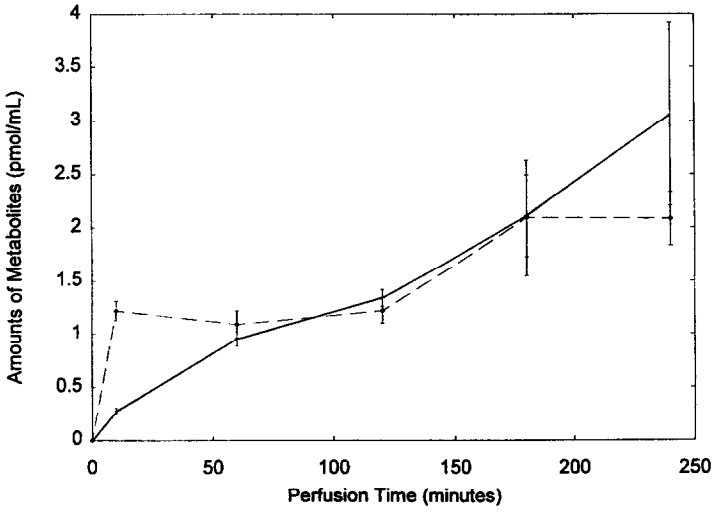

Fig. 8. Production rates of Δ^{16}1,24,25(OH)$_3$D$_3$ (broken line) and Δ^{16}1,25(OH)$_2$-24-oxo D$_3$ (solid line) in the rat kidney, based on MRM analysis of perfusate samples drawn from the 80 μg/100 mL perfusion experiment. Number of injections at each time point = 4. Values are means ± SD.

since the enzyme(s) involved in the C-24 oxidation pathway was not oversaturated under that situation.

Detection of vitamin D compounds in biological media by μLC-ESI MS/MS is both sensitive and specific. The derivatization with PTAD is selective for vitamin D-type compounds, and it increases the ESI detectability of the analytes. The resulting ion transition under CID from these derivatives is unique and highly selective. For trace level quantification, the more commonly used single ion monitoring technique may be slightly more sensitive than MRM, but it suffers from a severe lack of specificity when applied to the analysis of biological samples. By taking advantage of the unique ion transition observed for PTAD-derivatized vitamin D compounds, target analytes may be detected with higher specificity and confidence without sacrificing the sensitivity needed for trace level analysis. Similarly, the parent scan technique based on the same ion transition provides the necessary specificity for analysis in biological samples, while simplifying the screening process by identifying only vitamin D-type compounds. The on-line coupling of a μLC further enhances the sensitivity of this multi-dimensional analysis by preconcentrating the analytes prior to MS detection. Complete HPLC separation is not necessary as the detection of specific ion transitions by MS/MS suffices in distinguishing the individual analytes.

Besides sensitivity and selectivity, detection of vitamin D compounds by the techniques described here offers a further advantage in that both natural and synthetic vitamin D compounds can be detected, provided that the diene bonds at 5,6 and 10,19 positions are available for derivatization with PTAD. This point was demonstrated in the work reported here where the natural $1,25(OH)_2D_3$ and the synthetic $\Delta^{16}1,25(OH)_2D_3$ were both detected with equal sensitivities. Therefore, the μLC-ESI MS/MS technique can potentially overcome detection problems encountered with some synthetic vitamin D analogs that fail to bind efficiently with vitamin D binding protein or vitamin D receptor preparation in conventional radioreceptor protein binding assays.

Acknowledgements—Financial support for this work from USPHS Biomedical Support Grant RR07143 (P.V.) and NIH Grant DK-39138 (G.S.R.) is gratefully acknowledged. This is Publication No. 620 from the Barnett Institute.

REFERENCES

1. Napoli JL and Horst RL, Vitamin D metabolism. In: *Vitamin D: Basal Clinical Aspects* (Ed. Kumar R), pp. 91–123. Martinus Nijhoff, Boston, 1984.
2. Minghetti PP and Norman AW, $1,25(OH)_2$-Vitamin D_3 receptors: Gene regulation and genetic circuitry. *FASEB J* **2**: 3043–3053, 1988.
3. Walters MR, Newly identified actions of the vitamin D endocrine system. *Endocr Rev* **13**: 719–764, 1992.
4. Abe E, Miyaura C, Sakagami H, Takeda M, Konno K, Yamazaki T, Yoshiki S and Suda T, Differentiation of mouse myeloid leukemia cells induced by 1α,25-dihydroxyvitamin D_3. *Proc Natl Acad Sci USA* **78**: 4990–4994, 1981.
5. Kragballe K and Wildfang IL, Calcipotriol (MC 903), a novel vitamin D analogue, stimulates terminal differentiation and inhibits proliferation of cultured human keratinocytes. *Arch Dermatol Res* **282**: 164–167, 1990.
6. Zhou J-Y, Norman AW and Lubbert M, Novel vitamin D analogs that modulate leukemic cell growth and differentiation with little effect on either intestinal calcium absorption or bone calcium mobilization. *Blood* **74**: 82–93, 1989.
7. Zhou J-Y, Norman AW, Chen D-L, Sun G-W, Uskokovic M and Koeffler HP, 1,25-Dihydroxy-16-ene-23-yne-vitamin D_3 prolongs survival time of leukemic mice. *Proc Natl Acad Sci USA* **87**: 3929–3932, 1990.
8. Colston KW, Chander SK, MacKay AG and Coombes RC, Effects of synthetic vitamin D analogues on breast cancer cell proliferation *in vivo* and *in vitro*. *Biochem Pharmacol* **44**: 693–702, 1992.
9. Colston KW, MacKay AG and James SY, EB 1089: A new vitamin D analogue that inhibits the growth of breast cancer cells *in vivo* and *in vitro*. *Biochem Pharmacol* **44**: 2273–2280, 1992.
10. Binderup L, Latini S and Binderup E, 20-Epi-vitamin D analogues: A novel class of potent regulators of cell growth and immune responses. *Biochem Pharmacol* **42**: 1569–1575, 1991.
11. Bikle DD, Clinical counterpoint: Vitamin D: New actions, new analogs, new therapeutic potential. *Endocr Rev* **13**: 765–784, 1992.
12. Kragballe K, Vitamin D analogues in the treatment of psoriasis. *J Cell Biochem* **49**: 46–52, 1992.
13. Lowe KE and Norman AW, Vitamin D and psoriasis. *Nutr Rev* **50**: 138–142, 1992.
14. Binderup L, Immunological properties of vitamin D analogues and metabolites. *Biochem Pharmacol* **43**: 1885–1892, 1992.
15. Binderup L and Bramm E, Effects of a novel vitamin D analogue MC 903 on cell proliferation and differentiation *in vitro* and on calcium metabolism *in vivo*. *Biochem Pharmacol* **37**: 889–895, 1988.
16. Kissmeyer A-M and Binderup L, Calcipotriol (MC 903): Pharmacokinetics in rats and biological activities of metabolites. *Biochem Pharmacol* **41**: 1601–1606, 1991.
17. Sorensen H, Binderup L and Calverley MJ, *In vitro* metabolism of calcipotriol (MC 903), a vitamin D analogue. *Biochem Pharmacol* **39**: 391–393, 1990.
18. Jung SJ, Lee YY, Pakkala S, De Vos S, Elstner E, Norman AW, Green J, Uskokovic M and Koeffler HP, $1,25(OH)_2$-16-ene-Vitamin D_3 is a potent antileukemic agent with low potential to cause hypercalcemia. *Leuk Res* **18**: 453–463, 1994.
19. Reddy GS, Clark JW, Tserng KY, Uskokovic MR and McLane JA, Metabolism of $1,25(OH)_2$ 16-ene D_3 in kidney: Influence of structural modification of D-ring on side chain metabolism. *Bioorg Med Chem Lett* **3**: 1879–1884, 1993.
20. Lemire JM, Archer DC and Reddy GS, 1,25-Dihydroxy-24-oxo-16-ene-vitamin D3, a renal metabolite of the vitamin D analog 1,25-dihydroxy-16-ene-vitamin D3, exerts immunosuppressive activity equal to its parent without causing hypercalcemia *in vivo*. *Endocrinology* **135**: 2818–2821, 1994.
21. Yeung B, Vouros P and Reddy GS, Characterization of vitamin D_3 metabolites using continuous-flow fast atom bombardment tandem mass spectrometry and high performance liquid chromatography. *J Chromatogr* **645**: 115–123, 1993.
22. Yeung B, Reddy GS and Vouros P, Characterization of vitamin D_3 metabolites by static and dynamic fast atom bombardment tandem mass spectrometry. In: *Proceedings of the 40th ASMS Conference on Mass Spectrometry and Allied Topics, Washington, DC, May 31–June 5, 1992* (Ed. Marshall AG), p. 1089–1090. The American Society for Mass Spectrometry, East Lansing, MI, 1992.

23. Reddy GS, Jones G, Kooh SW and Fraser D, Inhibition of 25-hydroxyvitamin D_3-1-hydroxylase by chronic metabolic acidosis. *Am J Physiol* **243**: E265–E271, 1982.
24. Rhodes CJ, Claridge PA, Trafford DJH and Makin HLJ, An evaluation of the use of Sep-Pak C18 cartridges for the extraction of vitamin D_3, and some of its metabolites from plasma and urine. *J Steroid Biochem* **19**: 1349–1354, 1983.
25. Busch KL, Glish GL and McLuckey SA, *Mass Spectrometry/Mass Spectrometry: Techniques and Applications of Tandem Mass Spectrometry*. VCH Publishers, New York, 1988.
26. Reddy GS and Tserng K-Y, Calcitroic acid, end product of renal metabolism of 1,25-dihydroxyvitamin D_3 through C-24 oxidation pathway. *Biochemistry* **28**: 1763–1769, 1989.